European Journal of Forest Research, 2023
Author pre print - DOI : 10.1007/s10342-023-01565-w

From the simulation of forest plantation dynamics to the quantification of bark-stripping damage by ungulates

Gauthier Ligot[1]*, Thibaut Gheysen[2], Jérôme Perin [1], Romain Candaele [1], François de Coligny [4], Alain Licoppe [3], Philippe Lejeune [1]

Abstract
Large ungulate populations are known to cause economic damage to agriculture and forestry. Bark damage is particularly detrimental to the timber production of certain species, including *Picea abies* (L.) Karst. (Norway spruce): after bark is wounded, rot often spreads in the trunk base, damaging the most valuable trunk section. Numerous studies have provided valuable information on various aspects of this process but the financial consequences over a full timber production cycle remained poorly quantified and uncertain. To fill this gap, we coupled a forest dynamics model (GYMNOS) with models of damage occurrence and decay spread. We simulated the effect of ranging levels of bark-stripping damage on financial losses. The simulations were repeated for sites of ranging fertility and with different protection measures (fences or individual protections), in Southern Belgium. The net present values of these different simulations were estimated and compared to estimate the cost of the damage and the cost-effectiveness of the damage protections. Protecting plantations against bark-stripping damage with fences was found unlikely to be worthwhile. By contrast, individual protections placed on crop trees could be helpful, particularly in the most fertile stands. Loss of revenue depended greatly on the factors tested: we estimated that the average damage cost could be about 53€/ha/year, reducing timber yield by 19%. A model was built to predict the damage cost for different values of the discount rate, site index and bark-stripping rate. This model could help develop more effective management of Norway spruce plantations and deer populations.

[1] *Forest is Life, TERRA, Gembloux Agro-Bio Tech, Université de Liège, Belgique*
[2] *Département de la Nature et des Forêts, SPW ARNE, Gembloux, Belgium*
[3] *Département de l'Etude du Milieu Naturel et Agricole, SPW ARNE, Jambes, Belgium*
[4] *AMAP, niv. Montpellier, CIRAD, CNRS, INRAE, IRD, Montpellier, France*
***Corresponding author**: gligot@uliege.be

1. Introduction

Excessive ungulate densities are known to harm agricultural and forestry production (Ward et al., 2004). In the case of timber production, ungulates are known to browse seedlings, rub their antlers on tree trunks or strip the bark from young trees. Among such damage, bark-stripping by red deer (*Cervus elaphus* L.) is especially detrimental to certain tree species such as Norway spruce (*Picea abies*(L.) Karst.) whose bark is particularly sought after by red deer and whose damaged stems are especially prone to fungal infection and decay (Burņeviča et al., 2016; Cukor et al., 2022). Given that the density of large wild ungulates has substantially increased over the last century in temperate forests (Milner et al., 2006; Apollonio et al., 2010), the extent of this damage is of concern and deserves a rigorous quantification.

To date, the drivers and characteristics of bark-stripping damage on spruce trees have been relatively well described (Gill, 1992b; Vospernik, 2006; Candaele et al., 2021; Cukor et al., 2019a; Widén et al., 2022). We also have valuable information on the subsequent decay in the stems and well-detailed models of forest stand dynamics and forest management (Burņeviča et al., 2016; Čermák and Strejček, 2007; Vacek et al., 2020). However, combining all this knowledge to evaluate the impact of bark-stripping from planting through to final harvest at stand scale has rarely been undertaken and described (Čermák et al., 2004a). Therefore, it remains difficult to assess how to adapt forest management to different levels of bark-stripping damage.

The prevalence of bark-stripping damage is known to increase with ungulate density and depends on tree size, hunting management and environmental characteristics (Gill, 1992b; Candaele et al., 2021; Vospernik, 2006; Widén et al., 2022). Red deer mostly strip the bark of relatively young spruce trees as soon as the stem is stiff and accessible while the bark is still thin (Vospernik, 2006; Ligot et al., 2013). The prevalence of bark-stripping has been monitored using forest inventories in sensitive stands. In relatively large forest areas (over 1000 ha), typical values of annual bark-stripping rates range between 0 and 12% (Candaele et al., 2021). This rate is correlated to deer abundance but the relationship saturates beyond a certain ungulate density (Ligot et al., 2013; Candaele et al., 2021). The other factors that can affect the frequency of bark-stripping damage are winter harshness, forest composition, distance from roads and urban areas, canopy opening, availability of

other food resources such as beechnuts and acorns, and topographic position (Ligot et al., 2013; Candaele et al., 2021; Vospernik, 2006; Widén et al., 2022; Konôpka et al., 2022). The damage might occur both in winter and summer (Gill, 1992b; Widén et al., 2022). Nevertheless, in summer, the bark is more loosely attached to the stem, and so deer typically remove longer strips of bark than in winter. According to Gheysen et al. (2011), the strip can be twice as long in summer (30.2 cm in average) as in winter (15.6 cm).

After bark is damaged on spruce trees, wounded tissues are often infected by fungi, causing subsequent wood decay and discoloration (Löffler, 1973; Čermák et al., 2004a; Mäkinen et al., 2007; Burņeviča et al., 2016). Various decay-causing fungi have been identified; of which the most important one is *Stereum sanguinolentum*. After infection by *S. sanguinolentum*, a decay column forms around the wound (Burņeviča et al., 2016). The vertical spread of the decay depends on wound age, wound size, and various environmental factors. It varies greatly across studies (Löffler, 1973; Čermák et al., 2004a; Čermák and Strejček, 2007; Mäkinen et al., 2007). The spread is generally fast during the first years after infection but subsides after 20-30 years (Čermák et al., 2004a; Čermák and Strejček, 2007). The resulting height of the decay column can reach at most 4-6 m depending on the rate of decay spread and so on environmental conditions (Čermák et al., 2004a; Čermák and Strejček, 2007; Vacek et al., 2020). For example, Vacek et al. (2020) observed that stem rot reached maximum 4.5 m (mean = 1.9 m) at one site and maximum 6.0 m (mean = 3.1 m) at another site, in the Czech Republic.

A significant proportion of bark-stripped stems may contain decayed wood of low economic value. According to Vacek et al. (2020), the average proportion of decayed wood in damaged trees can range between 30% and 39%. Similar or even higher values were found in the Czech Republic (Čermák and Strejček, 2007; Čermák et al., 2004b) and in Belgium (Heyninck, 2014). Often, the trunk sections that contain decayed wood cannot be sawn and can be used only by pulp and paper industries. The value of these sections containing decayed wood is thus very limited (Heyninck, 2014).

These losses can be attenuated by forest management. In western Europe, spruce plantations are usually regularly thinned before the final cut (clear-cut). The damaged trees can then be thinned preferentially over the healthy trees (Vacek et al., 2020; Heyninck, 2014). However, in most cases, it is unrealistic to fell every damaged tree in one or a few thinnings because bark damage are often aggregated within stands (Hahn and Vospernik, 2022). Forest managers can protect stands against ungulate damage: plantations can be fenced, or individual trees can be protected by scarifying their trunks to stimulate resin flows (Fig. 3), fitting plastic sleeves or nets around their trunks, wrapping branches around their trunks, or using chemicals (Trout and Brunt, 2014). Individual protection can be installed, at about the time of the first thinning, on all trees or only on a selection of the most valuable trees that are expected to be harvested last (crop trees) (Perin et al., 2016).

Assessing the financial impact of bark-stripping damage on timber production is complex because it requires taking into account multiple variables and processes on a long time scale ($>$ 50 years). Consequently, most studies have focused on certain processes but rarely make a comprehensive assessments of financial losses (Gill et al., 2000) . Gill et al. (2000) illustrated how such an assessment could be made with elementary models, but acknowledged that their approach was limited and that further models had to be developed to estimate yield losses, particularly for Norway spruce. In line with what has been proposed to assess the economic impacts of browsing by roe deer (Ward et al., 2004; Rakotoarison, 2009) or moose (Wam and Hofstad, 2007), an assessment can be made by modeling forest dynamics and interactions with ungulate populations (Weisberg et al., 2003). Once models are established, they can be used to predict the costs and revenues of different management strategies in ranging treatment and/or environmental conditions (e.g., ungulate density).

To fill this gap, we coupled a model of the forest dynamics and management of even-aged coniferous stands with models of bark-stripping damage. We then conducted a virtual experiment to address several questions: Does bark-stripping damage substantially harm the profitability of Norway spruce plantations? Should rotation be shortened in the stands that are highly impacted by bark-stripping damage? Is it more cost-effective to protect plantations with fences or to protect individual trees against bark-stripping at the time of the first thinning (i.e., after some damage has already occurred)?

2. Materials and methods

2.1 Study area

Different data sets were collected in Southern Belgium (Wallonia, approx. 50° N, 5° E, Fig. 1), mostly in the Ardenne region. The climate in Southern Belgium is warm temperate, with no dry season and a mild summer (classified as Cfb in the Köppen-Geiger scheme). Elevation varies between 20 m and 700 m and is generally highest in Ardenne. Annual rainfall and mean annual temperature range respectively between 800 mm.year^{-1} and 10.5°C and 1400 mm.year^{-1} and 7.5°C (averages computed for 1981–2010 by the Belgian Royal Meteorology Institute). Annual rainfall are positively correlated to elevation whereas mean annual temperature are negatively correlated to elevation. The climate in Ardenne is thus colder and wetter than in the other areas of Wallonia. About 60% of the forest area of Wallonia is located in Ardenne. Norway spruce plantations cover around 26% of the total productive forest area. In 2016, they constituted 40% of the standing stock and 50% of the total wood production. Most of these plantations of Norway spruce (92%) are located in Ardenne (Lejeune et al., 2022). Spruce plantations are mostly found on brown acidic soil with sometimes poor drainage. They are normally thinned every 5–10 years once the top height reaches 13–20 m and are clearccut when the top height reaches 30 m (Perin et al., 2016).

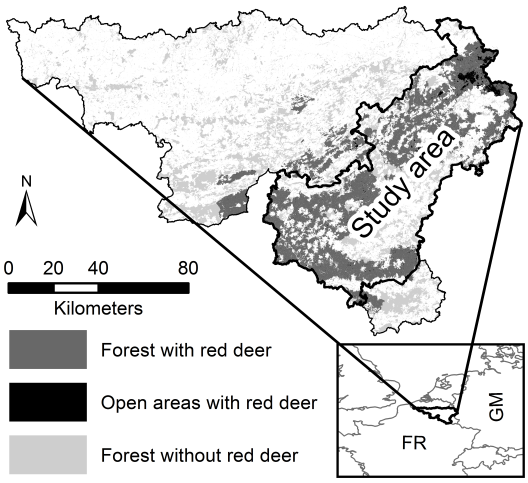

Figure 1. Map of the study area as illustrated by Candaele et al. (2021).

Red deer, the roe deer (*Capreolus capreolus*) and the wild boar (*Sus scrofa*) are the three native ungulate species living in the study area. Within the study area, the estimated density of red deer populations ranged between 0 and 16.5 animals/km^2 and the reported number of shot red deer ranged between 0 and 6.7 animals/km^2/year (Candaele et al., 2021). Roe deer or wild boar are also relatively abundant but their density cannot be accurately estimated (Candaele et al., 2021).

2.2 Bark-stripping inventory data

Since 2003, regional monitoring of bark-stripping damage has been carried out in the study area. This monitoring system has been described in detail by Gheysen et al. (2011) and Candaele et al. (2021). The sampling units were installed on the nodes of a 200 × 200 m sampling grid that fall into spruce plantations of 8-36 years old (Fig. 2a). In each samplig unit, three circular plots of up to 10 m radius were laid out on a north–south transect (Fig. 2b). In each plot, the six tree closest to the plot center were measured. The sampling units had been measured annually between mid-April and mid-May since 2003. Between 2004 and 2015, over 4,000 plots and 60,000 trees were measured each year (Candaele et al., 2021).

2.3 Models of forest dynamics and management

A model of forest stand dynamics was developed to simulate the evolution of mono-specific plantations of Norway spruce, Douglas-fir (*Pseudotsuga Menziesii* (Mirb.) Franco.) and larch (*Larix decidua* Mill. and *L. kaempferii* (Lamb.) Carrière) in Southern Belgium. This model, named GYMNOS, is an empirical distance-independent tree model of stand dynamics with an annual time step. It is implemented as a JAVA module in the open-source Capsis4 platform (Dufour-Kowalski et al., 2012). It includes equations and algorithms used to simulate stand initialization, top-height growth (Perin et al., 2013), individual tree growth (Perin et al., 2017), individual tree mortality and thinning (Table 1).

The model had previously been thoroughly tested and used to define reference sylvicultural scenarios such as local yield tables (Perin et al., 2016). The model is open-source and can be downloaded free (hdl.handle.net/2268/260468), for example to run simulations with different parameters (e.g., site index, plantation density or thinning date and intensity) from those we chose in this study.

2.3.1 Top-height growth

The growth of stand top-height, defined as the mean height of the 100 largest trees per hectare, is an important variable in our stand dynamics model. The evolution of stand top-height is predicted using the model of Perin et al. (2013) (Eq. 1). The top-height in a stand ($Hdom_y$) that is y years old is predicted knowing the top-height ($Hdom_{50}$) at 50 years. The top-height reached at 50 years is an indicator of site productivity called the site index (SI), and is used to define yield classes Perin et al. (2013). For instance, in sites of average fertility, the top-height of a spruce stand reaches approximately 27 m at 50 years of age. In this model, tree age is defined as the biological age of the trees (plantation age + planted seedling age assumed to be 4 years).

2.3.2 Stand initialization

At stand initialization, the girth at breast height of tree (gbh_i) is drawn from a log-normal distribution (Eq. 2) whose parameters depend on plantation density (N) and top-height ($Hdom$). To fit this model, we collected data about tree diameter in 332 additionnal plots of 50-1850 m^2 in even-aged stands of Norway spruce, Douglas-fir or larch ranging in age from 9 to 93 years.

The height of a tree (h_i) was estimated using a model depending on the mean girth of the 100 largest trees ($Gdom$), tree girth (gbh_i) and stand top-height ($Hdom$, Eq. 3). This model was fitted with another dataset containing records of tree diameter and height of 13,236 trees in 720 circular plots of 1018 m^2 located in even-aged stands of Norway spruce, Douglas-fir or larch ranging also in age from 9 to 93 years.

2.3.3 Growth

Tree growth is predicted using the model of Perin et al. (2017). Tree annual girth increment (Δgbh_i) depends on initial tree girth ($gbh_{i,y-1}$), initial stand top-height ($Hdom_{y-1}$), estimated top-height reached at the end of the year ($Hdom_y$) and initial stand basal area (BA_{y-1}). This model was calibrated for stands taller than 10 m in top-height. Under 10 m top-height, the annual girth increment (between year y and $y-1$) is derived from Eq. 2 computing the difference between μ values (Eq. 5). Once tree girth is updated, tree height increment is computed with Eq. 6 derived from Eq. 3.

2.3.4 Timber volume

The volume of trunk, from stump to the height of the section 7 cm in diameter, is predicted using local species-specific allometric relationships (Dagnelie et al., 2013) that depend on tree girth (gbh_i) and stand top-height ($Hdom$, Eq. 7).

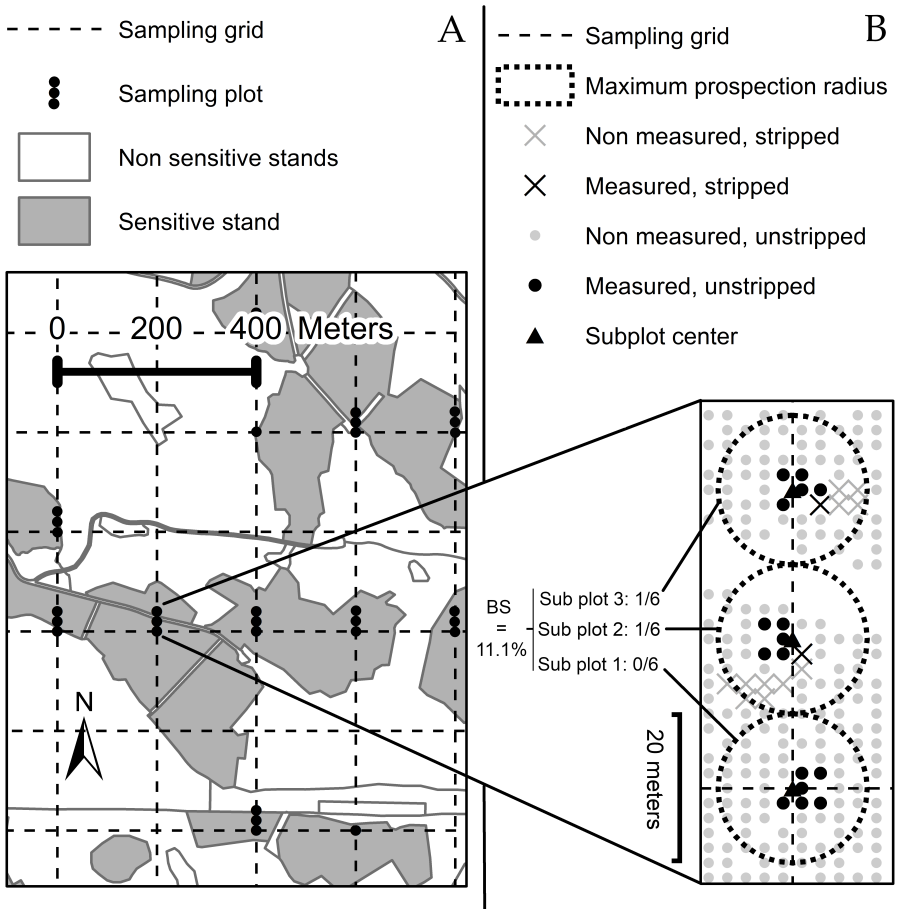

Figure 2. Design of the sampling method as illustrated by Candaele et al. (2021). The plots are installed on the nodes of a square grids that fall into Norway spruce plantations of 8-36 years old (sensitive stands, A). At each selected nodes, six trees were measured in three circular plots (B).

Table 1. Equations of the stand dynamics and bark-stripping damage. The symbols and abbreviations are described in table 2.

Process	Equation	
Top height	$Hdom_y = (0.130 \cdot age_y + bi) \cdot \left(1 - exp(-\frac{age_y}{22.4})\right)^{2.05}$	(1)
	$bi = \frac{Hdom_{50}}{(1 - exp(-(\frac{50}{22.4}))^{2.05}} - 0.130 \cdot 50$	
Stand initialization	$gbh_i \sim Log\text{-}\mathcal{N}(\mu, \sigma^2); \qquad \mu = 0.5 \cdot log(cg^2) - \sigma^2; \qquad \sigma = 0.0245 \cdot N^{0.317}$	(2)
	$cg = \left(\frac{40000 \cdot \pi \cdot 13.3 \cdot rdi}{N}\right)^{1/1.65}; \qquad rdi = 1 - exp(-2.61 \cdot 10^{-6} \cdot N \cdot Hdom^2)$	
H-D allometry	$h_i = 0.799 \cdot Hdom \cdot \arctan\left(\tan(\frac{1}{0.799}) \cdot \frac{gbh_i}{Gdom}\right)\left(\tan(\frac{1}{0.799}) \cdot \frac{gbh_i}{Gdom}\right)$	(3)
Girth growth ($h_i \geq 10$)	$\Delta gbh_i = (gbh_{i,y-1}^2 + \Delta g_i \cdot 4 \cdot \pi)^{0.5} - gbh_{i,y-1}$	(4)
	$\Delta g_i = \frac{P}{2} \cdot \left(gbh_{i,y-1} - M \cdot A + \left((M \cdot A + gbh_{i,y-1})^2\right) - 4 \cdot A \cdot gbh_{i,y-1}\right)^{0.5}\Big)$	
	$A = 3.98 \cdot Hdom_y^{0.780} \qquad P = 0.216 + 0.801 \cdot (Hdom_y - Hdom_{y-1})$	
	$M = 1 + \exp(0.135 \cdot Hdom_y - 0.185 \cdot BA_{y-1})$	
Girth growth ($h_i < 10$)	$\Delta gbh_i = \exp(\log(gbh_{i,y-1}) + \mu_{i,y} - \mu_{i,y-1}) + gbh_{i,y-1}$	(5)
Height growth	$\Delta h_i = 0.799 \cdot (Hdom_y - Hdom_{y-1}) \cdot \arctan\left(\tan(\frac{1}{0.799}) \cdot \frac{gbh_{i,y}}{Gdom_{y-1}}\right)$	(6)
Timber volume	$V_i = 0.0135 - 0.00128 \cdot gbh_i + 0.0000457 \cdot gbh_i^2 - 7.70 \cdot 10^{-8} . gbh_i^3$	(7)
	$-0.00114 \cdot Hdom + 2.58 \cdot 10^{-6} \cdot gbh_i^2 \cdot Hdom$	
Taper function	$g10_i = 5.36 + 1.07 \cdot gbh_i - 0.00194 \cdot gbh_i^2 + 7.47 \cdot 10^{-7} \cdot gbh_i^3$	(8)
	$-0.416 \cdot h_i + 2.86 \cdot 10^{-5} \cdot gbh_i^2 \cdot h_i$	
	$g_{h,i} = a_h + b_h \cdot g10_i + \frac{c_h}{g10_i^2}$	(9)
Tree mortality	$rdi = \frac{N}{N_{max}}; \qquad N_{max} = 40000 \cdot \pi \cdot 13.286 \cdot cg^{-1.65}$	(10)
	$rdi_{max} = rdi_{y-1} + (1 - \min(1, rdi_{y-1}^{8.5}))(rdi - rdi_{y-1}) - 0.5 \max(0, rdi_{y-1} - 1)$	(11)
	$s_i = u_i \cdot \frac{gbh_i - \min(gbh)}{\max(gbh) - \min(gbh)} \qquad u_i \sim U[0,1]$	(12)
Thinning	$s_i = S \cdot u_i + (1 - S) \cdot \frac{gbh_i - gbh^*}{m} \qquad u_i \sim U[0,1]$	(13)
	$gbh^* = T \cdot (\max(gbh) - \min(gbh)) + \min(gbh)$	
	$m = \max(gbh^* - \min(gbh), \max(gbh) - gbh^*) + 1$	
	$\frac{cut_{damaged}/N_{damaged}}{cut_{healthy}/N_{healthy}} = 1.5$	(14)
Bark-stripping rate	$\tau_{summer,s} = f_{summer}(age_s; \mu = 3.08, \theta = 0.194) \cdot \frac{BSR \cdot (36 - 8)}{0.854} \cdot 0.2$	(15)
	$\tau_{winter,s} = f_{winter}(age_s; \mu = 2.68, \theta = 0.440) \cdot \frac{BSR \cdot (36 - 8)}{0.950} \cdot 0.8$	(16)
Prob. of damage	$P(\text{being damaged}, i) = 0.0144 \cdot dbh_i \cdot exp(-0.125 \cdot dbh_i) + \varepsilon_i$	(17)
	$\varepsilon_i \sim \mathcal{N}(0, 5.27 \cdot 10^{-3})$	
Decay spread	$dl = \exp(0.769 + 0.336 \cdot \log(Ks) + 0.150 \cdot \log(w) + 0.605 \cdot \log(l)$	(18)
	$+0.336 \cdot \log(p) + 0.545 \cdot \log(rw))$	

Table 2. Symbols and abbreviations.

Symbols	Description
age	Stand age
$Hdom_y$	Stand top height at y years of age (m)
$Hdom_{50} = SI$	Site index, stand top height at y years of age (m)
N	stand density (trees/ha)
gbh_i	Girth of tree i at 1.3 m (cm)
dbh	Tree diameter at 1.3 m (cm)
Δgbh_i	Annual girth increment of tree i (cm/year)
cg	Quadratic mean of tree girth (cm)
rdi	Stand density index
N_{max}	Maximum tree density (trees/ha)
rdi_{max}	Maximum stand density index
$Gdom$	Mean girth of the 100 largest trees/ha (cm)
BA_y	Stand basal area at year y (m^2/ha)
$g10_i$	Tree girth at 10% of tree heigth (cm)
g_h	Tree girth at h m (cm)
a_h, b_h, c_h	Fitted parameters of the taper equation
T	Thinning type
S	Thinning stochastic coefficient
s_i	Score of tree i used in the thinning algortithm
$cut_{damaged}$	Density of damaged thinned trees (trees/ha)
$cut_{healthy}$	Density of healthy thinned trees (trees/ha)
$N_{healthy}$	Stand density of healthy trees, before thinning (trees/ha)
$N_{damaged}$	Stand density of damaged trees, before thinning (trees/ha)
BSR	Bark-stripping rate
f_{summer}	Summer damage probability function
f_{winter}	Winter damage probability function
$\tau_{summer,s}$	Summer bark-stripping rate in stand s
$\tau_{winter,s}$	Winter bark-stripping rate in stand s
ε_i	Model residual
dl	Length of the decay column (cm)
Ks	Tree Kraft status, social position
w	Damage width (cm)
l	Damage length (cm)
p	Time elapsed since the damage (years)
rw	Mean ring width (mm)
μ	Distribution mean
θ	Distribution standard deviation
NPV	Net present value over a finite (n years) time horizon (€/ha)
NPV_∞	Net present value over an infinite time horizon (€/ha)
r	Discount rate

The volume of decayed wood resulting from bark-stripping damage is computed using local allometric equations (Dagnelie et al., 1985). First, the girth at a reference height level (10% of tree height, $g10_i$) is computed (Eq. 8).

Then, the girth at different height levels (g_h) is computed with equation 9. The chosen height levels were 10, 50, 130, 250, 350 cm in height and 30% of tree height. In this equation, the parameters a_h, b_h and c_h depends on the chosen height level and they were calibrated by Dagnelie et al. (1985).

Using these estimates, the girth at any height can be estimated by linear interpolation. The volume of the base of a trunk is estimated by summing the volume of successive trunk sections and assuming that their shape is a truncated cone (Rondeux, 1999).

2.3.5 Mortality

Mortality is modeled using a self-thinning curve defining the maximum tree density (N_{max}) observed in a stand of a given quadratic mean girth (cg) and yields a relative density index (rdi, Eq. 10).

The conventional approach consists in simulating mortality once $rdi > 1$. However, this approach led to simulations with unrealistically large rdi values and abrupt changes in stand density. A smooth function, depending on the initial stand rdi (rdi_{y-1}), was therefore developed to simulate mortality in a more gradual way (Eq. 11). Using this approach, tree mortality is simulated so long as stand rdi is greater than rdi_{max}.

To determine which trees die, a score s_i is computed for every tree (Eq. 12). Trees are sorted according to this score and the algorithm sequentially removes the trees with the lowest scores so long as $rdi > rdi_{max}$. The score includes a stochastic term u_i, whose values are drawn from a uniform distribution bounded between 0 and 1.

2.3.6 Thinning algorithm

Thinnings are defined by values of thinning intensity, thinning types and a stochastic coefficient. The thinning intensity corresponds to a target value of stand density, standing volume or relative density index (rdi). The thinning type (T) ranges between 0 and 1 and translates a forester's preference for harvesting small or large trees. Thinning whose types is 0, 1, and 0.5 harvest respectively the smallest trees, the largest trees and trees of intermediate girth (gbh^*). The stochastic coefficient (S) also ranges between 0 and 1 and indicates the amount of added random noise. If $T = 0$ and $S = 0$, then only the smallest trees are harvested whereas if $S = 1$ then the trees are harvested independently of tree size. The algorithm computes a score s_i for each tree, and sequentially harvests the tree with the lowest s_i (Eq. 13) until thinning intensity is reached.

This algorithm was further improved to account for the presence of trees with bark-stripping damage because foresters may preferentially thin damaged trees over healthy ones. Using additionnal data measured in 59 thinned stands (10,882 trees) where the proportion of bark-stripping damage ranged

between 8% and 99%, we found that the forester's preference for harvesting damaged trees was best modeled by computing the mean odds ratio between damaged and healthy trees (Eq. 14). To ensure that this odds ratio is maintained in the simulation, the thinning algorithm is applied first on damaged trees and secondly on healthy trees with adapted thinning intensities.

Crop trees can be selected and protected against bark-stripping damage at the time of the first thinning. These trees are, if possible, not harvested before the final cut. The crop trees were selected preferentially among healthy large trees using the same algorithm as that used to simulate thinnings with $S = 0.3$ and $T = 1$.

2.4 Models of bark-stripping damage

The abundance of bark-stripping damage is modulated by one variable: the average bark-stripping rate observed at the landscape scale (*BSR*). This rate is defined as the average proportion of healthy or damaged trees presenting new (maximum 1 year-old) damage, in stands 8-36 years old. It is the main indicator that can be computed from bark-stripping inventories (Section 2.2). Assuming the forest landscape to be composed of pure even-aged spruce stands of ranging age, it is reasonable to assume that ungulates preferentially gather in stands of a certain age that provide adequate food resources and shelter. The bark-stripping rate at the stand level will then vary with stand age. We assumed that bark-stripping rate was nil at age 0, peaked at an intermediate age and was very low in old stands. Like Candaele et al. (2021) using the same bark-stripping inventory data, we assumed that the proportion of the bark-stripping rate of winter and summer damage peaked, respectively, in stands 21 and 12 years old. In addition, we assumed that only 5% of total bark stripping damage occurred in stands younger than 8 years and older than 36 years. This assumption seemed reasonable because most damage has been observed, in different independent studies, in stands 8-36 years old (Vospernik, 2006; Jerina et al., 2008; Gill et al., 2000; Konôpka et al., 2022). With these assumptions (distribution modes, proportion of damage in stands 8-36 years old), we computed the parameters of the two corresponding probability density functions (f_{summer} and f_{winter} in Eq. 15 and 16). These distributions are used to distribute the damage among stands depending on their age. To simulate the amount of damage corresponding to a chosen *BSR*, the damage probability functions are multiplied by a first coefficient ($C = BSR / \int_8^{36} f(x) \cdot dx$). The result is then multiplied by a second coefficient to ensure that the proportions of summer and winter damage are 20% and 80%, respectively, and to compute the rates of summer and winter new bark-stripping damage ($\tau_{summer,s}$ and $\tau_{winter,s}$).

Next, to assign this damage among the trees of one stand, we used the data of bark-stripping inventories to model the probability of a tree being damaged according to its diameter (*dbh*, Eq. 17). This probability was used to compute a score for every tree. The damage was assigned to the trees with the highest score. We note that it contains a stochastic term ε_i drawn from a normal distribution.

From 2003 to 2005, the positions and sizes of 1820 summer damage instances and 9955 winter damage instances were recorded. Based on these records, the height, width, and length of winter and summer damage wounds were estimated. The damage width and height were not significantly different between summer and winter. However, the summer damage wounds were generally longer (Gheysen et al., 2011). The distribution of damage height, width, and length was modeled with Weibull and log-normal distributions (Table 3).

After damage, decay can spread around the wound. As decay generally spread in the majority of the damaged stem (Metzler et al., 2012; Gill, 1992a), we made the simplistic assumption that decay developed in 100% of the damaged stems. Additionally, the rate of decay spread was modeled using the model of Löffler (1973). This model was developed for Norway spruce in Germany. It predicts the length of the decay column (*dl*) as a function of the tree Kraft status (*Ks*), damage width (*w* in cm), damage length (*l* in cm), time elapsed since the damage (*p* in years) and mean ring width (*rw* in mm). The tree Kraft status is a discrete variable used to measure tree social status (Kraft, 1884). It ranges between 1 (dominant tree) and 5 (suppressed tree).

Here also, very different models have been proposed (Čermák et al., 2004a,b; Čermák and Strejček, 2007). We verified that the length of the simulated decay column was consistent with local field observations at the final cut, i.e., with column decay being generally shorter than 3 m and very rarely reaching 4 m (Gheysen T., pers. comm.).

2.5 Simulation scenarios

We simulated the even-aged sylviculture of Norway spruce stands following the local guidelines previously adjusted using the same forest stand dynamics model and through a long iteration process with field experts (Perin et al., 2016).

The simulated plantation density was 2000 trees/ha, of which 90% were expected to survive until the first thinning. The first thinning was simulated 17, 19, 22, 25 or 29 years after the plantation in sites whose site index (*SI*) is 33, 30, 27, 24 or 21 m, respectively. The type of all simulated thinnings (T in Eq. 13) is 0.15. The first thinning reduced stand density to 1280 trees per hectare with a stochastic coefficient fixed at $S = 0.692$. Before the first thinning, the trees are pruned to a height of 2 m as it is usually done in the study area to ease tree marking. The second, third and subsequent thinnings reduced stand *rdi* to 0.49, 0.53 and 0.55 with $S = 0.3$. The thinnings were simulated every 6 years which is the usual cutting cycle length for spruce stands in the study area.

Four protection treatments were tested : without any protection ("the unprotected treatment"), protecting all trees individually at the first thinning ("bark-scraping all"), selecting and protecting 400 crop trees/ha at the first thinning ("bark-scraping 400"), and protecting all trees with a fence (erected at plantation, "the fence treatment"). Different meth-

Table 3. Distribution parameters of bark-stripping damage height, width and length.

Variables	Season	Distribution	Parameter ± std. error	
Height (cm)	All	$Weibull(k, \delta)$	4.692 ± 0.034	112.421 ± 0.232
Width (cm)	All	$Log\text{-}\mathcal{N}(\mu, \theta^2)$	1.582 ± 0.006	0.634 ± 0.004
Length (cm)	Summer	$Log\text{-}\mathcal{N}(\mu, \theta^2)$	2.834 ± 0.022	0.922 ± 0.015
Length (cm)	Winter	$Log\text{-}\mathcal{N}(\mu, \theta^2)$	2.236 ± 0.007	0.704 ± 0.005

ods have been proposed to protect trees individually against bark-stripping damage : lattice sleeve, bark protection net and bark scraping. All these protections are usually implemented at the time of the first thinning and generally after pruning. The last solution, bark-scraping, was the cheapest and the most frequently implemented in the study area at the time of writing this manuscript, and so this solution was selected. It consists in scraping the bark generally with a Gerstner plane. The scraping must be light so as not to damage the cambium while stimulating a resin flow (Fig. 3). This solution might, however, not be as effective as more costly ones (Ueckermann et al., 1988).

Simulations were carried out for stands using five values of site index (21, 24, 27, 30, 33 m), 11 values of bark-stripping rates (*BSR*) ranging between 0 and 10% and four protection treatment levels. As the model included stochastic terms, for each combination, 5 repetitions were simulated leading to 1,100 simulations.

2.6 Financial assessment

The financial losses caused by bark-stripping damage were assessed by quantifying the costs (C) and revenues (R) of timber production during a full rotation. The revenues and costs of hunting activities were not considered.

The revenues were computed by multiplying the merchantable volume of trunks (up to a diameter of 7 cm) by unit prices. The volume of the decayed trunk sections was computed using local allometric relationships (Section 2.3.4) and the height reached by the column decay (Section 2.4). The timber unit prices were computed using data of the public sales of timber in 2021 in Southern Belgium. Of all sales, we selected 499 public sales (426,986 m^3 in total) whose volume comprised at least 85% of Norway spruce. We excluded sales originating from sanitary cuts. The unit price was then estimated by girth class (Table 4) (Sanchez et al., 2004). The unit price for the decayed trunk sections could not be estimated with public sale records and it was set at 5€/m^3, the estimated market price (FNEF, 2022).

The costs considered were those usually incurred following plantation of Norway spruce in Southern Belgium. The costs of the plantation and subsequent operations are given in Table 5. The cost of fencing a 1 ha plantation was set at 6000 €. The cost of bark-scraping a tree to protect it against bark-stripping was set at 1.34 €/tree.

Figure 3. Within the study area, spruce trees are often protected from bark damage by ungulates by lightly scraping (e.g. with a Gerstner plane) the bark to stimulate a resin flow. The scars remain visible during several years.

Table 4. Timber price by girth class estimated from public timber sales in 2021, in Southern Belgium.

Girth class (cm)	Price (€/m^3)
< 40	0.0
$[40-50[$	3.3
$[50-60[$	14.9
$[60-70[$	25.4
$[70-80[$	35.0
$[80-90[$	43.6
$[90-100[$	51.2
$[100-110[$	57.8
$[110-120[$	63.4
$[120-130[$	68.0
$[130-140[$	71.6
$[140-150[$	74.2
$[150-160[$	75.8
$[160-170[$	76.4
$[170-180[$	76.0
$[180-190[$	74.6
$[190-200[$	72.2
> 200	68.8

Table 5. Costs common to all simulation scenarios.

Cost	Year	Price (€/ha)
Plantation	0	2400
Weeding	1	640
Weeding	3	640
Weeding	5	640
Pruning	17	1219

For each simulation, the cash flows were summarized by computing the net present value (NPV_∞, Eq. 19) which, for a given discount rate (r), is the difference between the discounted revenues and costs over an infinite time horizon. If the NPV_∞ is greater than zero, then the discounted revenues are greater than the discounted costs and that the investment generates profits. Different rotation lengths were tested and the selected optimum rotation length was the one maximizing NPV_∞. The tested rotation lengths corresponded to the different thinning dates (Section 2.5), i.e., every 6 years from the first thinning to 100 years.

$$\begin{aligned} NPV &= \frac{\sum_{i=0}^{n} R_{(i)} - C_{(i)}}{(1+r)^i} \\ NPV_\infty &= NPV. \frac{(1+r)^n}{(1+r)^n - 1} \end{aligned} \tag{19}$$

The opportunity cost of bark-stripping damage, i.e. the discounted loss due to bark-stripping damage, was computed with the unprotected simulations as $NPV_{\infty,BSR=0} - NPV_\infty$, where $NPV_{\infty,BSR=0}$ was the average of NPV_∞ for the simulations with the same site index and $BSR = 0\%$. To discuss the magnitude of the opportunity costs, we computed the corresponding annuities by multiplying the opportunity costs by the discount rate. Such annuities can be interpreted as the amount that need to be paid annually to offset the cost of the bark-stripping damage.

These computations critically depend on the discount rate, which is the key variable to estimate the discounted (or present) value of future cash flows. For such projects, there is still scant agreement on what the appropriate rate might be (Gollier and Hammitt, 2014). We therefore avoided a single value and we repeated the computations with different rates (1%, 2%, 3% and 4%).

In addition, we verified that computing the opportunity cost of bark-stripping damage over a single rotation (i.e. computing the difference between NPV rather than between NPV_∞) led to the same conclusions whatever the discount rate, and barely affected our estimates of the opportunity cost (Suppl. Table S1).

2.7 Statistical analyses

Simulation results were mostly compared visually because the differences were generally well marked. Even so, some models were fitted to synthesize the results.

The relationships between the opportunity cost of bark-stripping damage in response to stand site index, discount rate, and bark-stripping rate was modeled with a linear model whose intercept was zero and whose slope depended on the discount rate and site index (Eq. 20).

$$\text{Opportunity cost} = (\beta_1 + \beta_2 \cdot r + \beta_3 \cdot SI) \cdot BSR \tag{20}$$

Similarly, the NPV_∞ was modeled with a linear model whose intercept and slope depended on the site index, discount

rate, bark-stripping rate and protection treatment denoted T in Eq. 21.

$$NPV_\infty = (\alpha_{1,T} + \alpha_2 \cdot SI + \alpha_3 \cdot r) + (\beta_{1,T} + \beta_2 \cdot r) \cdot BSR \quad (21)$$

3. Results

3.1 Stand characteristics over time

Over the 100 simulated years, the main characteristics of the simulated stands depended primarily on site index (*SI*) and little on treatment or bark-stripping rate (Fig. 4). For a given site index, the timber volume productivity and, the intensity and type of the thinnings were thus very similar across the treatments and bark-stripping rates. Trees grew faster in the most productive site with a high site index. At stand initialization (i.e. at 8 year old), the mean tree diameter ranged between 3.2 cm ($SI = 21$ m) and 6.0 cm ($SI = 33$ m). Mean productivity ranged between 11.7 m^3/ha/year ($SI = 21$ m) and 17.9 m^3/ha/year ($SI = 33$ m).

The number of trees with bark-stripping damage increased with bark-stripping rate (*BSR*) depending also on the treatment and plantation age (Fig. 5). The number of bark-stripped trees generally peaked in 25-year-old stands and then slowly declined as the damaged trees were thinned. For example, in unprotected stands with $SI = 27$ m, the proportion of damaged trees was about 31% and 81% with $BSR = 2\%$ or 8%, respectively.

At clear-cut, the number of trees containing decayed wood increased with the bark-stripping rate and depended on the treatment (Fig. 6). When the bark-stripping rate was low (e.g. $BSR = 2\%$), most of the harvested trees were healthy (Fig. 5) but the proportion of harvested trees with damage increased sharply with *BSR*. In unprotected plantations, at least half of the harvested trees were damaged if $BSR \geq 5\%$ and more than 80% of trees were damaged if $BSR \geq 10\%$.

At clear-cut, the height of the decay column in the damaged trees ranged between 0.6 m and 5.6 m with an average of 2.1 m (Fig. 6C). This variability resulted mostly from the stochastic terms of the models used to predict the damage dimensions (Section 2.4).

3.2 Losses in timber volume and value

For all treatments except fencing, the total volume of harvested undamaged trunk sections (during thinnings and clear-cut) decreased with bark-stripping rate (Fig. 7). The reduction was obviously stronger in unprotected plantations than in plantations with individual protections. The volume of undamaged trunk section was very similar in the two scenarios with individual protections (bark-scraping all and bark-scraping 400).

Individual protections were installed at the first thinning. As the first thinnig occured later in the stands of low productivity (low site index), individual protection were installed later in the low productivity stand than in the high productivity stand. In the low productivity stands, the proportion of damaged trees could then already be high when individual protections were applied (bark-scraping all and bark-scraping 400). The effect of these protections thus became limited (Suppl. Fig. S2).

3.3 Net present value

3.3.1 Optimum rotation time

The optimum rotation value varied substantially with the site index (*SI*), discount rate (r), and bark-stripping rate (*BSR*, Suppl. Fig. S1). Optimum rotation was shorter for the most productive sites (high site index) and/or when using a high discount rate. For example, when $r = 2\%$ and $BSR = 0\%$, the mean optimum rotation was 65.6 and 96.3 years in stands with $SI = 33$ m and $SI = 21$ m, respectively.

The optimum rotation also depended, though to a lesser extent, on the interaction between the treatment and the bark-stripping rate. For example, when $r = 2\%$, $BSR = 0\%$ and $SI = 27$ m, the optimum rotation was 76 years in unprotected stands and 82 years in fenced stands. In the same conditions but with $BSR = 10\%$, the optimum rotation did not differ between treatments (Suppl. Fig. S1, 82 years for all treatment). Generally, the optimum rotation tended to be longer when the bark-stripping rate was high. When the bark-stripping rate was low, the optimum rotation of fenced stands was longer than that in the other scenarios. The opposite was nevertheless observed when bark-stripping rate was high and discount rate low.

Moreover, combining a low site index ($SI = 21$) m and a low discount rate ($r = 1\%$) gave an optimum rotation that was longer than the tested ones (100 years, Suppl. Fig. S1). An optimum rotation of 100 years was nevertheless considered for these cases.

3.3.2 Opportunity cost of bark-stripping damage

The opportunity cost of bark-stripping damage ranged between 0 and 19,445 €/ha. For example, with $r = 2\%$, in unprotected stands of average fertility ($SI = 27$ m), the net present value was about 16,492 €/ha if no damage occurred (*BSR*=0%). It fell to 11,048 €/ha with the highest simulated level of damage (*BSR*=10%) as the opportunity cost was 5,443 €/ha (i.e., 37% of NPV_∞ without damage).

The opportunity cost of bark-stripping damage depended on the bark-stripping rate, discount rate, and site index (Fig. 8). More precisely, the opportunity cost increased linearly with bark-stripping rate, and the slope of this relationship increased with the site index and decreased with the discount rate (Table 6). The opportunity cost expressed in absolute value increased with site index while its the relative value decreased with site index (Fig. 8, 9 and Suppl. Fig. S5).

3.3.3 Net present value across treatments

The net present value increased with site index, decreased with discount rate, and varied across treatments. When no damage occurred ($BSR = 0\%$), the net present value of the fenced treatment was lowest ($\alpha_{1,f} - \alpha_{1,u} = -7.651 \cdot 10^3$, $p < 0.001$, Table 7) and the net present values of the scenarios with individual protections were only slightly, and not significantly

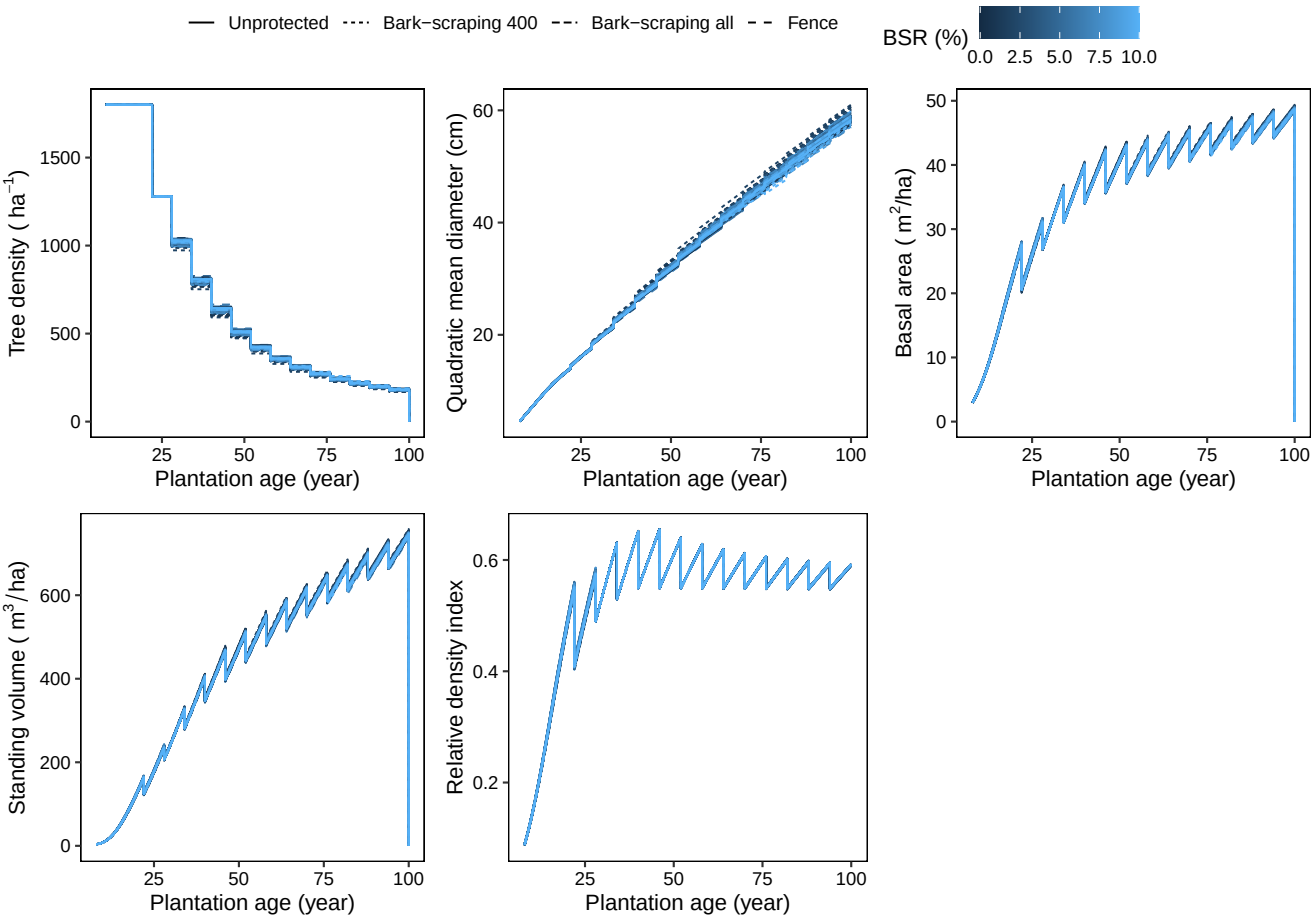

Figure 4. Changes in the main characteristics of the simulated stands: density, mean quadratic diameter, basal area, standing volume and relative density index (*rdi*). For clarity, only the simulations with averaged productivity stands are shown ($SI = 27$ m).

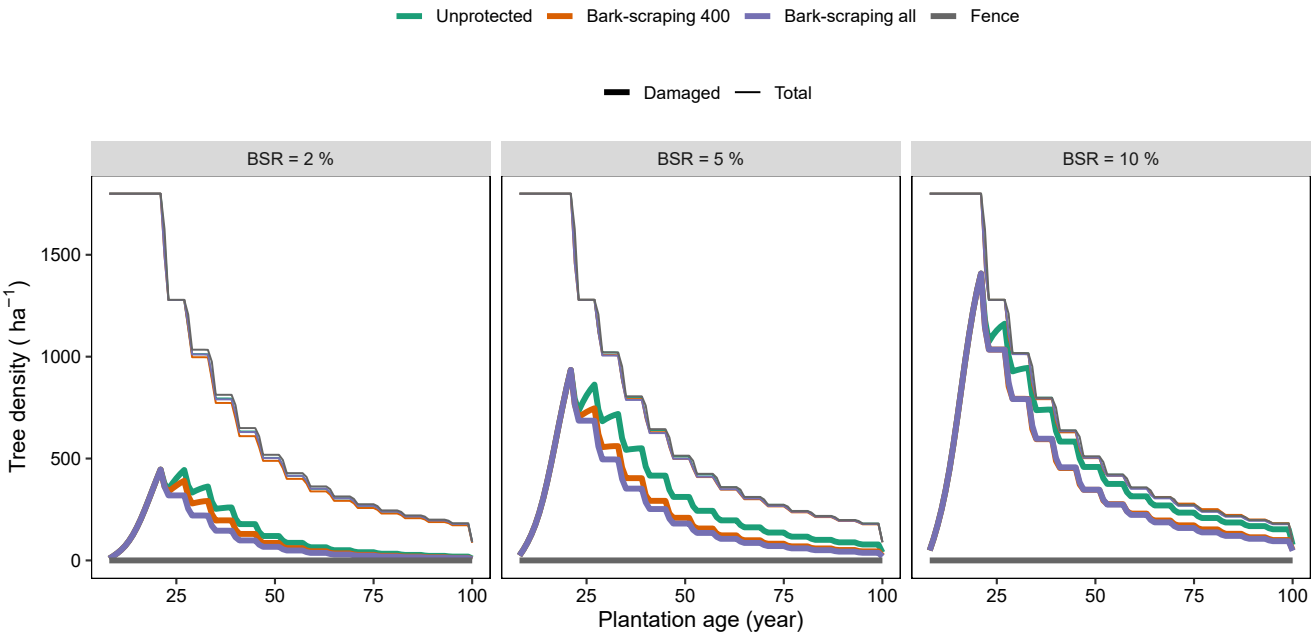

Figure 5. Changes in the mean stand density and density of damaged trees over time and for the different protection treatments. For clarity, only the simulations with averaged productivity stands are shown ($SI = 27$ m).

Table 6. Parameter estimates, standard errors and p-value of the fitted linear model of the opportunity cost of bark-stripping damage (Eq. 20) in response to the bark-stripping rate (BSR), site index (SI) and discount rate (r).

Param.	Effect	Estimate	Std. error	p
β_1	BSR	$1.05 \cdot 10^5$	$5.43 \cdot 10^3$	< 0.001
β_2	$BSR \cap r$	$-4.75 \cdot 10^6$	$7.13 \cdot 10^4$	< 0.001
β_3	$BSR \cap SI$	$3.10 \cdot 10^3$	$1.88 \cdot 10^2$	< 0.001

lower than that of the unprotected treatment (e.g. $\alpha_{1,s4} - \alpha_{1,u} = -1.373$, $p = 0.860$, Fig. 10).

The net present value decreased linearly with the bark-stripping rate for most treatments ($\beta_{1,u} = -1.308 \cdot 10^5$, $p < 0.001$) except for the fenced treatment, which was obviously unaffected by the bark-stripping rate (Table 7, Fig. 10 and Suppl. Fig. S3). For all scenarios except fencing, the slopes of this relationship varied little across treatments when the discount rate was low ($r = 0.01\%$), whereas the slopes of the unprotected scenario were markedly steeper than that of the other scenarios when the discount rate was high ($r \geq 0.03\%$, Fig. 10, Table 7).

The net present value of the fence scenario was higher than that of the other scenarios only when $r = 1$, $SI < 27$ and $BSR > 5\%$. The scenarios with individual protections had a higher net present value than the unprotected scenario when $SI \geq 27$m. The difference between these scenarios increased with r (Fig. 10, Suppl. Fig. S3).

4. Discussion

4.1 Model assumptions

Modeling such a complex system inevitably entails making simplistic assumptions, but, it allows hypotheses to be tested while controlling many factors. In particular, our simulations did not allow for any changes in the growth or mortality of Norway spruce trees due to climate change or any other disturbances (Cukor et al., 2019a; Šņepsts et al., 2022). The models of tree growth and mortality were calibrated with empirical data collected between 1971 and 2010 in healthy pure softwood plantations. However, such plantations have been increasingly affected by climate change, warmer temperatures, bark beetle outbreaks (Jönsson et al., 2009) and droughts (Lévesque et al., 2013). Nevertheless, the extent of such damage could be reduced if spruce is progressively replaced by other tree species and if winters become milder (Ligot et al., 2013; Candaele et al., 2021; Konôpka et al., 2022). The combined effects of climate changes and changes in forest structure and composition need to be addressed and clarified in future studies.

Bark-stripping is one only type of damage caused by ungulate populations. Other damage can be expected when ungulates are abundant. Browsing of juvenile trees and antler rubbing on tree trunks can further reduce timber yield (Ward et al., 2004). In this work, the cost of this additional damage was considered constant, although we could expect it to

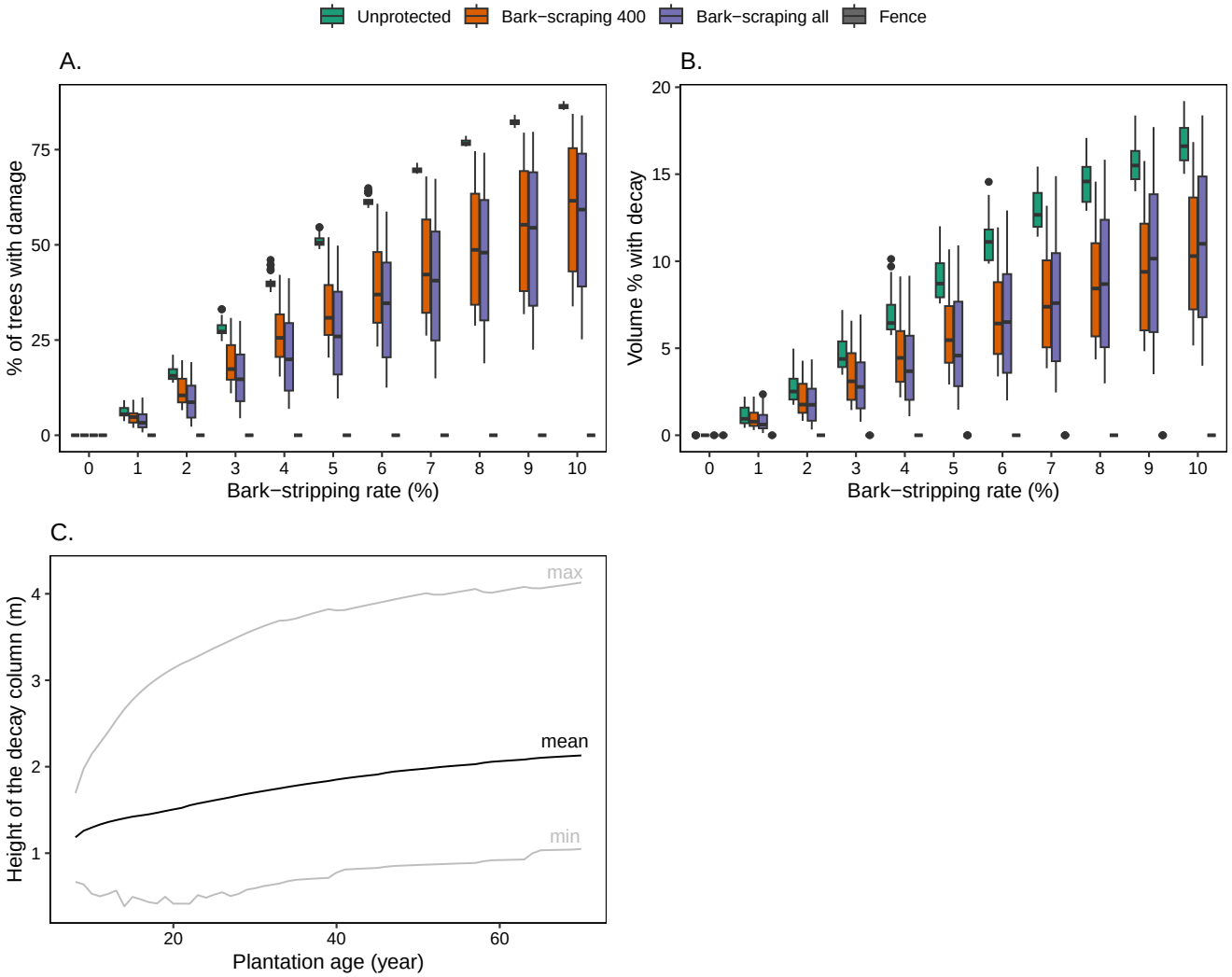

Figure 6. Predictions of decay spread and proportion of damaged trees across simulations. The top two plots show the variability in the percentage of trees (A) or stand volume (B) containing decayed wood at the final harvest and across treatments. At the bottom (C), the plot shows the evolution of the mean, minimum, and maximum heights of the decay column for the simulations without protection and with $BSR = 5\%$ and $SI = 27$ m.

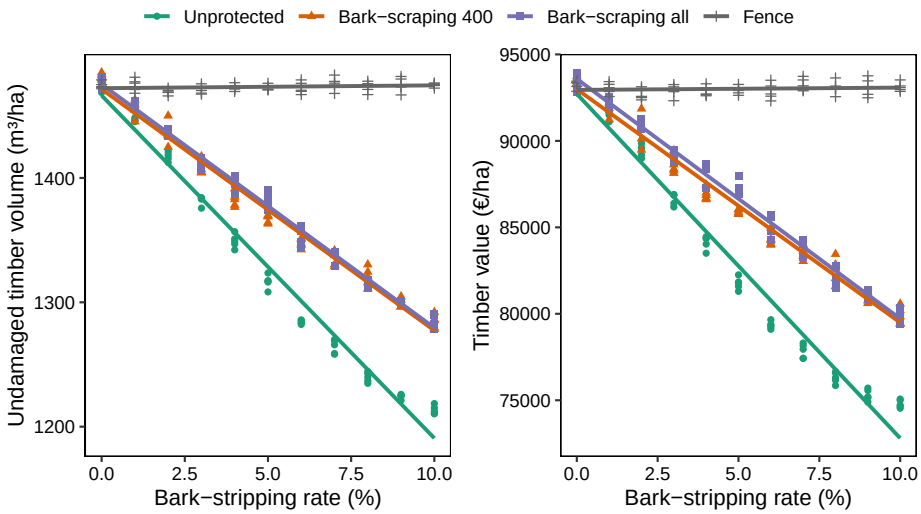

Figure 7. Undamaged volume and value of the trees thinned and harvested across treatments and bark-stripping rates. For clarity, only the simulations with averaged productivity stands are shown ($SI = 27$m).

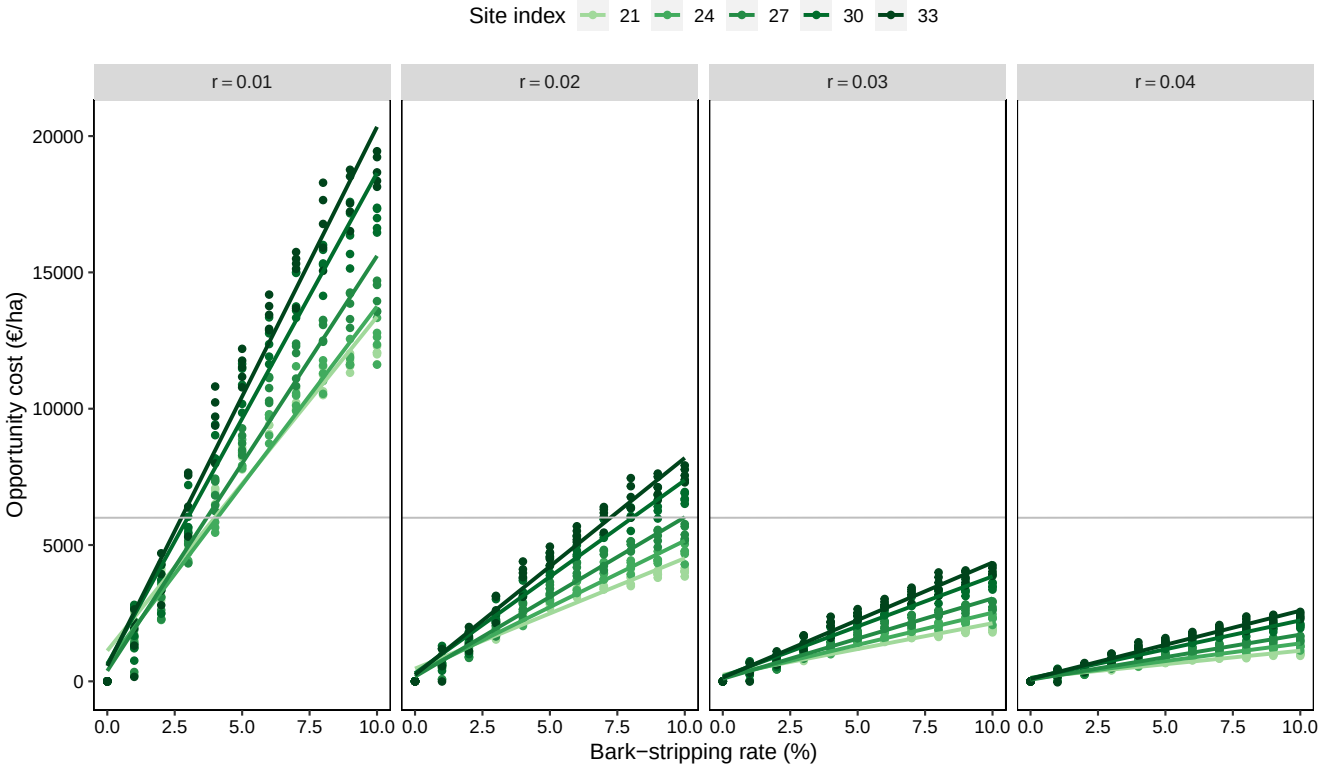

Figure 8. Relationships between the opportunity cost of bark-stripping damage, bark-stripping rate, discount rate and site index. The gray line indicates the estimated fencing cost (6000€/ha) incurred to protect all young trees from bark-stripping damage. The opportunity cost of bark-stripping damage is generally lower than the fencing cost except when the discount rate is very low.

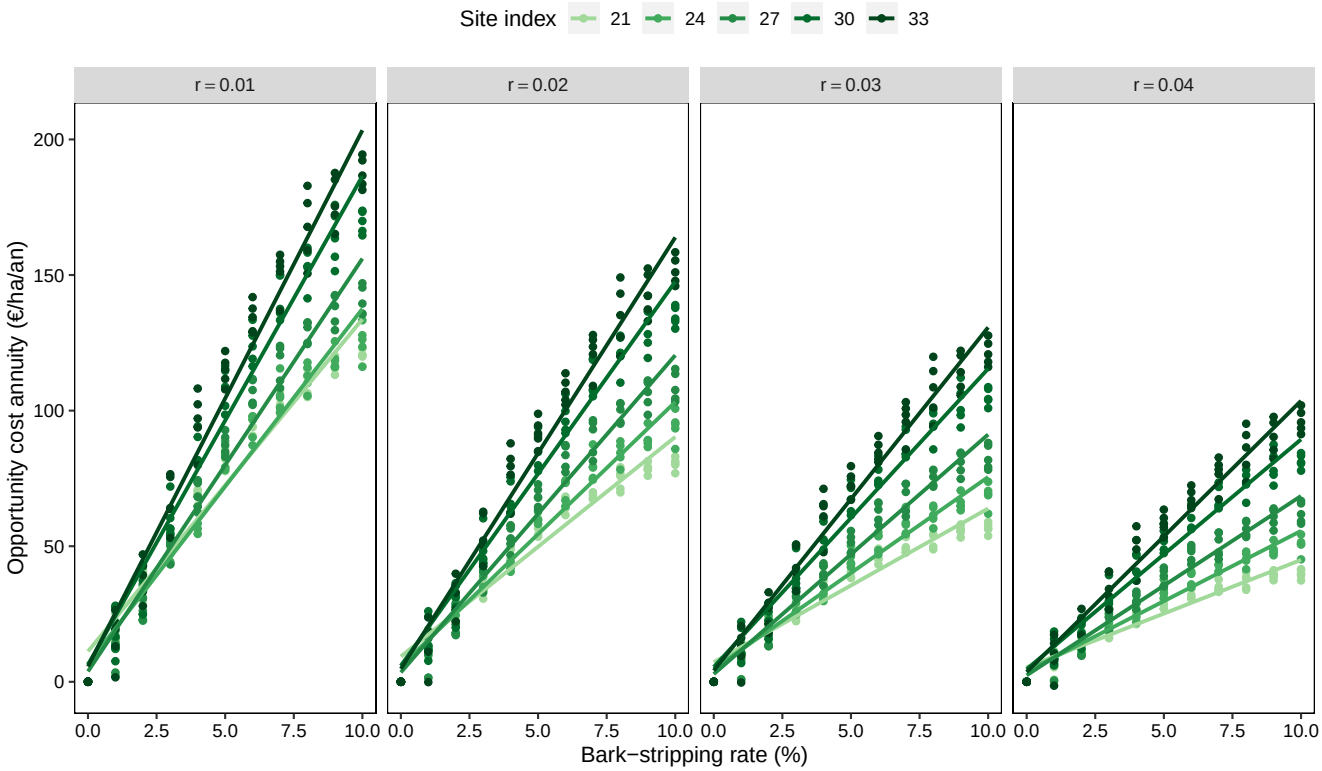

Figure 9. Relationships between the annuity of the opportunity cost of bark-stripping damage, bark-stripping rate, discount rate, and site index.

Table 7. Parameter estimates, standard errors, and p-values of the fitted linear model of the net present value (NPV_∞, Eq. 21) in response to the bark-stripping rate (BSR), site index (SI), discount rate (r), and protection treatment. The levels of the protection treatment are denoted u for the unprotected treatment, s for bark-scraping of all trees, $s4$ for bark-scraping of 400 crop trees/ha, and f for fencing. The symbol $\cap$ indicates an interaction between two explanatory variables.

Parameter	Effect	Estimate	Std. error	p
$\alpha_{1,u}$	Treatment	$2.468 \cdot 10^4$	$1.245 \cdot 10^3$	< 0.001
$\alpha_{1,s4} - \alpha_{1,u}$	Treatment	$-1.373 \cdot 10^2$	$7.762 \cdot 10^2$	0.860
$\alpha_{1,s} - \alpha_{1,u}$	Treatment	$-1.216 \cdot 10^3$	$7.762 \cdot 10^2$	0.117
$\alpha_{1,f} - \alpha_{1,u}$	Treatment	$-7.651 \cdot 10^3$	$7.762 \cdot 10^2$	< 0.001
α_2	SI	$1.463 \cdot 10^3$	$3.457 \cdot 10^1$	< 0.001
α_3	r	$-1.764 \cdot 10^6$	$2.454 \cdot 10^4$	< 0.001
$\beta_{1,u}$	BSR	$-1.308 \cdot 10^5$	$1.392 \cdot 10^4$	< 0.001
$\beta_{1,s4} - \beta_{1,u}$	$BSR \cap$ Treatment	$2.041 \cdot 10^4$	$1.312 \cdot 10^4$	0.198
$\beta_{1,s} - \beta_{1,u}$	$BSR \cap$ Treatment	$2.540 \cdot 10^4$	$1.312 \cdot 10^4$	0.053
$\beta_{1,f} - \beta_{1,u}$	$BSR \cap$ Treatment	$6.569 \cdot 10^4$	$1.312 \cdot 10^4$	< 0.001
β_2	$r \cap BSR$	$2.596 \cdot 10^6$	$4.149 \cdot 10^5$	< 0.001

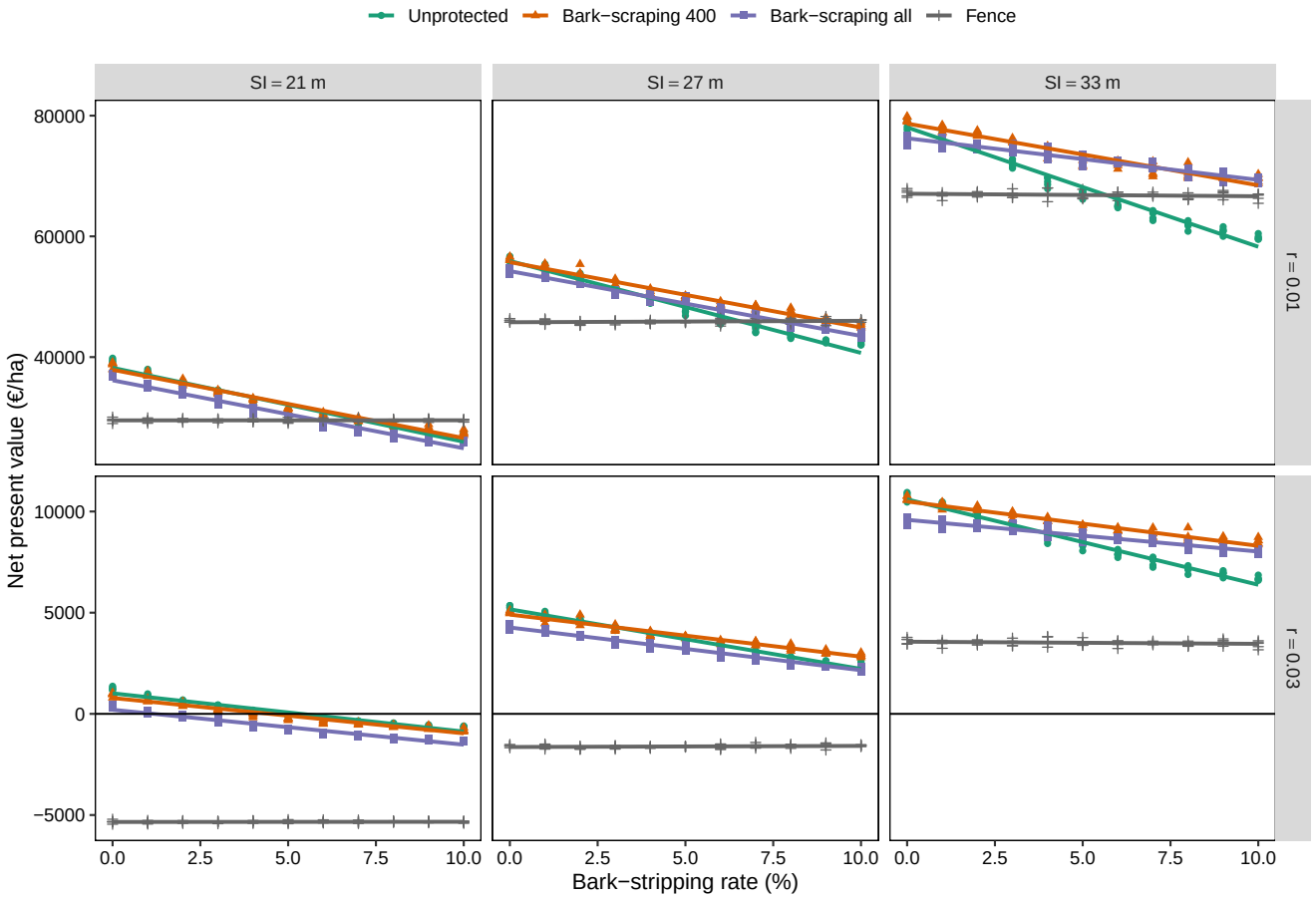

Figure 10. Variability of the net present value of the different scenarios across simulations with different bark-stripping rate, discount rate, and site index.

increase with bark-stripping rate. The cost of bark-stripping damage is thus only one component of the total cost of ungulate damage.

Additionally, we considered that bark-stripping damage and the associated decay would not affect tree growth or survival. While the vast majority of damaged trees survive, very rare exceptions can occur when the bark is removed over the entire stem circumference on small trees and in highly impacted areas (Gill et al., 2000). Furthermore, contrasting effects of bark-stripping damage on tree growth have been reported in the literature. These effects depend on wound size and position (Gill, 1992a; Mäkinen et al., 2007). It seems likely that a growth reduction can be observed in a damaged tree, but such growth reduction may be limited (except when the wound is very large) to a period of about 10 years after the wounding (Gill et al., 2000; Cukor et al., 2019b) and can ultimately be negligible (Gill et al., 2000). However, damaged stems can have reduced mechanical resistance (Čermák et al., 2004a; Šņepsts et al., 2022). Bark damage impairs tree hydraulics and may induce physiological drought and increase tree susceptibility to drought (Cukor et al., 2019b,a; Vacek et al., 2020), bark-beetle attacks, and wind damage (Snepsts et al., 2020; Šņepsts et al., 2022; Krisans et al., 2020).

We assumed that very few bark-stripping damage occurred in plantations younger than 8 years old (the simulations started in stands 8 years old) in line with several studies (Vospernik, 2006; Jerina et al., 2008; Gill et al., 2000; Konôpka et al., 2022). At 8 years old, the mean tree diameter ranged between 3.2 cm ($SI = 21$m) and 6.0 cm ($SI = 33$m), and so it seems reasonable to assume that bark-stripping damage seldom occurs on such small trees because their stem will not be stiff or accessible enough (Gill et al., 2000). Furthermore, in the study area, all trees in spruce plantations are generally pruned to a height of 2 m before the first thinning, and this operation, which is carried out earlier in the most productive stands, may hypothetically affect the behavior of ungulates. Nevertheless, we simulated damage occurrence without taking pruning into account because its effect is still poorly documented.

We also assumed that rot developed in all bark-stripping wounds, although it could develop in a smaller proportion of the wounded stems. This may have resulted in an overestimation of the losses induced by bark-stripping damage. The proportion of the wounds in which rot develops ranges widely across studies and environmental conditions. In a literature review, Gill (1992a) estimated this range at between 73.0% and 99.7%. Similar values were recently found in Germany (Metzler et al., 2012, 93%) but lower values were found in Latvia (Burņeviča et al., 2016, 13-50%) and in the Czech Republic (Čermák and Strejček, 2007, 68%). The rate of infection probably depends on wound size and environmental conditions (Vasaitis et al., 2012; Vasiliauskas, 2001; Cukor et al., 2019a). Although, infection was assumed to occur in every wound, the decay spread was modeled taking into account wound size and environmental conditions (Löffler, 1973). This model was deemed valid in the study area, but according to other studies carried out in different environmental conditions, the decay may spread slightly faster (Čermák et al., 2004a; Čermák and Strejček, 2007).

4.2 How badly does bark-stripping harm timber production and profitability?

The cost of bark-stripping damage can be substantial. It ranged between 0 and over 100% depending mostly on the rate of bark-stripping damage, discount rate, and, to a lesser extent, site index (Fig. 8 and Suppl. Fig. S3). With high bark-stripping rate ($BSR = 10\%$) and without protection, around 85% of the trees harvested at the final cut contained decayed wood and the volume of this decayed wood accounted for 15% of stand volume. According to Vacek et al. (2020) and Heyninck (2014), for one damaged tree, the decayed wood volume could instead account for 30-40 % of stem volume. These studies using other methodological approaches thus suggest that our predictions of the decayed wood volume at the stand level could be underestimated. However, the study of Vacek et al. (2020) was conducted on younger spruce stands in the Czech Republic and the study of Heyninck (2014) analyzed a very small sample of Norway spruce stems ($n = 17$) in a single site in Belgium.

Our results can be used to estimate the average cost of bark-stripping in the study area, making assumptions about the average bark-stripping rate, site index, and discount rate. Within the study area,the mean bark-stripping rate is about 4% (Gheysen et al., 2011). This rate also corresponds to the damage rate tolerated by the forest administration. In Southern Belgium, Norway spruce yields 14.7 m^3/ha on average, which corresponds to a site index of 27 m. If we choose a discount rate of $r = 2\%$, which seems reasonable for a project maturing over 50 years (Gollier and Hammitt, 2014), the average opportunity cost of bark-stripping damage will be 2647 €/ha which corresponds to an annuity of 53 €/ha/year. These figure are high, corresponding to a loss of net revenue of 19%. This cost is also of the same order of magnitude as the plantation costs or hunting leases.

Cost also depends on site fertility. Like Gill et al. (2000) for Sitka spruce plantations, we found that the relative cost of bark-stripping damage was greater in the least productive stands (Suppl. Fig. S5). In the most productive stands, the relative cost was lower, but the absolute cost was nevertheless higher (Fig. 8). For example, with BSR=4% and r =2%, the opportunity cost was about 2391 €/ha (35 % of NPV_∞) in the least productive stands and 3880 €/ha (17 %) in the most productive stands (with SI=33 and 21 m).

With our virtual experiment, we made a comprehensive assessment of the cost of bark-stripping damage over a full cycle of timber production. In particular, using Eq. 20 and the fitted parameters (Table 6), we can predict the opportunity cost of bark-stripping damage for any given values of the discount rate, site index and bark-stripping rate. Such information can be particularly helpful in making the management of Norway spruce plantations and deer populations more effective (Ward

et al., 2004).

4.3 How should forest management be adapted?

4.3.1 Rotation should be kept unchanged or only slightly lengthened

Forest managers may be tempted to shorten the rotation in stands where bark-stripping damage is observed because they are eager to start a new rotation. However, we found that the optimum rotation should either remain the same or be only slightly lengthened (e.g., 6 years more, Suppl. Fig. S1) irrespective of the discount rate used. In old stands, new bark-stripping damage becomes less likely (Vospernik, 2006; Jerina et al., 2008; Gill et al., 2000) and the spread of the decay is very low (Čermák et al., 2004a; Čermák and Strejček, 2007; Löffler, 1973). Considerations about the rotation length should therefore first take into account the effects of the discount rate, site index and certainly also, though not examined here, the risk of future disturbance to stands (Zimová et al., 2020) and other forest ecosystem services (Sing et al., 2018).

4.3.2 Cheap protections can still be helpful

Fencing to protect trees against bark-stripping damage is unlikely to be cost-effective. In most cases, its cost was appreciably greater than the opportunity cost of the damage (Fig. 8, 10 and Suppl. Fig. S3). Moreover, we probably underestimated its cost (6000 €/ha) because the fence maintenance costs were not counted. Fences in forests usually last about 15 years, much less than the time trees need protection against bark-stripping damage (about 40 years) (Gill et al., 2000). Fences were cost-effective only when the chosen discount rate was low ($r \leq 1\%$), the bark-stripping rate high and/or likley when saplings need also to be protected from browsing (Jensen et al., 2012).

Cheaper protections might be cost-effective particularly in the most productive stands. In this study, we assumed that such individual protections were placed at the time of the first thinning (at 17-29 years of age) (Perin et al., 2016). At that time, the trees are big enough to be pruned and their bark scraped to protect them against bark-stripping. Nevertheless, a substantial proportion of the trees may already be damaged at that age (Gill, 1992b; Candaele et al., 2021; Vospernik, 2006). In the simulations with high bark-stripping rates, individual protections could be fitted on already damaged trees, so having no effect or a very small effect on future timber value. This occurred mostly in the less productive stands and when the bark-stripping rate was very high ($BSR > 7\%$, Suppl. Fig. S4). In the most productive stand, the first thinning occurs earlier (Perin et al., 2016), and enough healthy crop trees can probably be found making individual protection a valid solution. In less fertile stands, individual protection should be fitted several years before the first thinnings.

5. Conclusion

Levels of wild ungulate populations have usually been adjusted to the damage levels, with limited regard to the actual cost of such damage. The model we propose in this study can be used to assess the cost of bark-stripping damage balancing long-term revenues against short-term costs of protection measures and long-term costs of bark-stripping damage. Knowing the true cost of bark-stripping damage is essential to improving the economic efficiency of deer and forest management. Protecting plantations against bark-stripping damage with fences was found unlikely to be worthwhile. By contrast, individual protections placed on crop trees could be helpful, particularly in the most fertile stands. Loss of revenue depended greatly on the factors tested: we estimated of the average damage cost could be about 53€/ha/year, reducing timber yield by 19%. Bark-stripping is one of the several factors affecting the proffitablity of Norway spruce plantations. To properly guide forest management, the other factors (e.g. browsing, changing environmental conditions, pest outbreak) that sometimes interact with bark-stripping should also be considered. The barkstripping damage should also be further investigated for unevenaged and mixed stands.

Declarations

Funding

The study was funded by the public service of Wallonia (SPW) under the funding: “Accord-cadre de recherches et vulgarisation forestières” (ACRVF 2009-2014 and 2014–2019).

Availability of data and material

An archive ZIP file containing the data generated by the simulations, an R scripts, and a read-me text file are available in the supplementary materials.

Code availability

The model is open-source and can be downloaded (hdl.handle.net/2268/260468).

References

Apollonio, M., Andersen, R., and Rory, P., 2010. *European ungulates and their management in the 21st century*. Cambridge University Press.

Burņeviča, N., Jansons, A., Zaluma, A., Klavina, D., Jansons, J., and Gaitnieks, T., 2016. Fungi inhabiting bark stripping wounds made by large game on stems of *Picea abies* (L.) Karst. in Latvia. *Baltic Forestry*, 22(1):2–7.

Candaele, R., Lejeune, P., Licoppe, A., Malengreaux, C., Brostaux, Y., Morelle, K., and Latte, N., 2021. Mitigation of bark stripping on spruce: the need for red deer population control. *Eur. J. For. Res.*, 140(1):227–240. ISSN 1612-4677. doi: 10.1007/s10342-020-01326-z.

Cukor, J., Vacek, Z., Linda, R., Sharma, R. P., and Vacek, S., 2019a. Afforested farmland vs. forestland: Effects of bark stripping by Cervus elaphus and climate on production potential and structure of Picea abies forests. *Plos One*, 14 (8). ISSN 1932-6203. doi: 10.1371/journal.pone.0221082.

Cukor, J., Vacek, Z., Linda, R., Vacek, S., Marada, P., Šimůnek, V., and Havránek, F., 2019b. Effects of bark stripping on timber production and structure of Norway spruce forests in relation to climatic factors. *Forests*, 10 (320):1–21. doi: 10.3390/f10040320.

Cukor, J., Vacek, Z., Linda, R., Vacek, S., Šimůnek, V., Macháček, Z., Brichta, J., and Prokůpková, A., 2022. Scots pine (Pinus sylvestris L.) demonstrates a high resistance against bark stripping damage. *For. Ecol. Manage.*, 513. doi: 10.1016/j.foreco.2022.120182.

Dagnelie, P., Palm, R., Rondeux, J., and Thill, A., 1985. *Tables de cubage des arbres et des peuplements forestiers*. Les presses agronomiques de Gembloux, Gembloux, Belgium.

Dagnelie, P., Palm, R., and Rondeux, J., 2013. *Cubage des arbres et des peuplements forestiers : Tables et équations*. Les Presses Agronomiques de Gembloux.

Dufour-Kowalski, S., Courbaud, B., Dreyfus, P., Meredieu, C., and De Coligny, F., 2012. Capsis: an open software framework and community for forest growth modelling. *Ann. For. Sci.*, 69(2):221–233. doi: 10.1007/s13595-011-0140-9.

Šņepsts, G., Krišāns, O., Matisons, R., Seipulis, A., and Jansons, r., 2022. Cervid bark-stripping is an explicit amplifier of storm legacy effects in Norway spruce (*Picea abies* (L.) Karst.) stands. *Forests*, 13(11):1947. doi: 10.3390/f13111947.

Čermák, P. and Strejček, M., 2007. Stem decay by *Stereum sanguinolentum* after red deer damage in the Českomoravská vrchovina Highlands. *J. For. Sci.*, 53(12): 567–572. doi: 10.17221/2164-JFS.

Čermák, P., Glogar, J., and Jankovský, L., 2004a. Damage by deer barking and browsing and subsequent rots in Norway spruce stands of forest range Mořkov, forest district Frenštát p. R.(the Beskids protected landscape area). *J. For. Sci.*, 50 (1):24–30. doi: 10.17221/4597-JFS.

Čermák, P., Jankovský, L., and Glogar, J., 2004b. Progress of spreading *Stereum sanguinolentum* (Alb. et Schw.: Fr.) Fr. wound rot and its impact on the stability of spruce stands. *J. For. Sci.*, 50(8):360–365. doi: 10.17221/4662-JFS.

FNEF, 2022. Liste des prix moyens de bois sur pied. Technical report, Jambes, Belgium. URL `https://www.experts-forestiers.be/Tableauprixbois.pdf`.

Gheysen, T., Brostaux, Y., Hébert, J., Ligot, G., Rondeux, J., and Lejeune, P., 2011. A regional inventory and monitoring setup to evaluate bark peeling damage by red deer (*Cervus elaphus*) in coniferous plantations in Southern Belgium. *Environ. Monit. Assess.*, 181(1):335–345. ISSN 0167-6369. doi: 10.1007/s10661-010-1832-6.

Gill, R., Webber, J., and Peace, A., 2000. The economic implications of deer damage: a review of current evidence. Technical report, Forest Research Agency, Surrey.

Gill, R. M. A., 1992a. A review of damage by mammals in North temperate forests: 3. Impact on trees and forests. *Forestry*, 65(4):363–388. doi: 10.1093/forestry/65.4.363-a.

Gill, R. M. A., 1992b. A review of damage by mammals in North temperate forests .1. Deer. *Forestry*, 65(2):145–169. doi: 10.1093/forestry/65.2.145.

Gollier, C. and Hammitt, J. K., 2014. The long-run discount rate controversy. *Annual Rev. Ressour. Economics*, 6:273–295. ISSN 1941-1340. doi: 10.1146/annurev-resource-100913-012516.

Hahn, C. and Vospernik, S., 2022. Position, size, and spatial patterns of bark stripping wounds inflicted by red deer (*Cervus elavus* L.) on Norway spruce using generalized additive models in Austria. *Ann. For. Sci.*, 79(13):1–16. doi: 10.1186/s13595-022-01134-y.

Heyninck, C., 2014. Pertes en volume et en valeur d'épicéas adultes touchés par des dégâts de cervidés. *Forêt Wallonne*, 132:24–30.

Jensen, A. M., Götmark, F., and Löf, M., 2012. Shrubs protect oak seedlings against ungulate browsing in temperate broadleaved forests of conservation interest: A field experiment. *For. Ecol. Manage.*, 266:187–193. doi: 10.1016/j.foreco.2011.11.022.

Jerina, K., Dajčman, M., and Adamič, M., 2008. Red deer (*Cervus elaphus*) bark stripping on spruce with regard to spatial distribution of supplemental feeding places. *Zbornik gozdarstva in lesarstva*, 86:33–43.

Jönsson, A. M., Appelberg, G., Harding, S., and Bärring, L., 2009. Spatio-temporal impact of climate change on the activity and voltinism of the spruce bark beetle, *Ips typographus*. *Global Change Biol.*, 15(2):486–499. doi: 10.1111/j.1365-2486.2008.01742.x.

Konôpka, B., Šebeň, V., Pajtík, J., and Shipley, L. A., 2022. Influence of tree species and size on bark browsing by large wild herbivores. *Plants*, 11(21):2925. doi: 10.3390/plants11212925.

Kraft, G., 1884. *Beiträge zur lehre von den durchforstungen, schlagstellungen und lichtungshieben*. Klindworth.

Krisans, O., Saleniece, R., Rust, S., Elferts, D., Kapostins, R., Jansons, A., and Matisons, R., 2020. Effect of bark-stripping on mechanical stability of Norway spruce. *Forests*, 11(357):1–8. doi: 10.3390/f11030357.

Lejeune, P., Michez, A., Perin, J., Gilles, A., Latte, N., Ligot, G., Lisein, J., and Claessens, H., 2022. L'épicéa wallon: état de la ressource en 2021. *Silva Belgica*, 2:16–23.

URL https://orbi.uliege.be/handle/2268/290618.

Löffler, H., 1973. Zur ausbreitung der wundfäule in der fichte. *Forstw. Cbl.*, 94:175–183.

Ligot, G., Gheysen, T., Lehaire, F., Hébert, J., Licoppe, A., Lejeune, P., and Brostaux, Y., 2013. Modeling recent bark stripping by red deer (*Cervus elaphus*) in south Belgium coniferous stands. *Ann. For. Sci.*, 70(3):309–318. ISSN 1286-4560. doi: 10.1007/s13595-012-0253-9.

Lévesque, M., Saurer, M., Siegwolf, R., Eilmann, B., Brang, P., Bugmann, H., and Rigling, A., 2013. Drought response of five conifer species under contrasting water availability suggests high vulnerability of Norway spruce and European larch. *Global Change Biol.*, 19(10):3184–3199. doi: 10.1111/gcb.12268.

Metzler, B., Hecht, U., Nill, M., Brüchert, F., Fink, S., and Kohnle, U., 2012. Comparing Norway spruce and silver fir regarding impact of bark wounds. *For. Ecol. Manage.*, 274: 99–107. doi: 10.1016/j.foreco.2012.02.016.

Milner, J. M., Bonenfant, C., Mysterud, A., Gaillard, J.-M., Csányi, S., and Stenseth, N. C., 2006. Temporal and spatial development of red deer harvesting in Europe : biological and cultural factors: red deer harvesting in Europe. *J. App. Ecol.*, 43(4):721–734. ISSN 00218901, 13652664. doi: 10.1111/j.1365-2664.2006.01183.x.

Mäkinen, H., Hallaksela, A.-M., and Isomäki, A., 2007. Increment and decay in Norway spruce and Scots pine after artificial logging damage. *Can. J. For. Res.*, 37(11):2130–2141. doi: 10.1139/X07-087.

Perin, J., Claessens, H., Lejeune, P., Brostaux, Y., and Hébert, J., 2017. Distance-independent tree basal area growth models for Norway spruce, Douglas-fir and Japanese larch in Southern Belgium. *Eur. J. For. Res.*, 136(2):193–204. doi: 10.1007/s10342-016-1019-y.

Perin, J., Hébert, J., Brostaux, Y., Lejeune, P., and Claessens, H., 2013. Modelling the top-height growth and site index of Norway spruce in Southern Belgium. *For. Ecol. Manage.*, 298:62–70. ISSN 0378-1127. doi: 10.1016/j.foreco.2013.03.009.

Perin, J., Hébert, J., Lejeune, P., and Claessens, H., 2016. De nouvelles normes sylvicoles pour les futaies pures équiennes d'épicéa et de douglas en appui à la gestion de la forêt publique en Wallonie. *Forêt.Nature*, 139:57–67.

Rakotoarison, H., 2009. *Analyse et modélisation de la gestion du grand gibier: cas de la région aquitaine*. PhD thesis, Université Montesquieu - Bordeaux IV.

Rondeux, J., 1999. *La mesure des arbres et des peuplements forestiers*. Les presses agronomiques de Gembloux, Gembloux. ISBN 2-87016-060-7.

Sanchez, C., Hebert, J., and Rondeux, J., 2004. Analyse des prix de ventes des bois en forêts publiques. *Forêt Wallonne*, 73:30–34.

Sing, L., Metzger, M. J., Paterson, J. S., and Ray, D., 2018. A review of the effects of forest management intensity on ecosystem services for Northern European temperate forests with a focus on the UK. *Forestry*, 91(2):151–164. doi: 10.1093/forestry/cpx042.

Snepsts, G., Kitenberga, M., Elferts, D., Donis, J., and Jansons, A., 2020. Stem damage modifies the impact of wind on Norway spruces. *Forests*, 11(463):1–15. doi: 10.3390/f11040463.

Trout, R. and Brunt, A., 2014. Protection of trees from mammal damage. *Forest Research, Best Practice Guidance for Land Regeneration*, 12:1–7.

Ueckermann, E., Orthwein, D., and Ueckermann, D., 1988. Modifizierung der mechanisch-biologischen Maßnahmen zum Schälschutz der jüngsten Fichtenaltersstufe. *Zeitschrift für Jagdwissenschaft*, 34(1):36–46.

Vacek, Z., Cukor, J., Linda, R., Vacek, S., Šimůnek, V., Brichta, J., Gallo, J., and Prokůpková, A., 2020. Bark stripping, the crucial factor affecting stem rot development and timber production of Norway spruce forests in Central Europe. *For. Ecol. Manage.*, 474:1–12. doi: 10.1016/j.foreco.2020.118360.

Vasaitis, R., Lygis, V., Vasiliauskaite, I., and Vasiliauskas, A., 2012. Wound occlusion and decay in *Picea Abies* stems. *Eur. J. For. Res.*, 131(4):1211–1216. doi: 10.1007/s10342-011-0592-3.

Vasiliauskas, R., 2001. Damage to trees due to forestry operations and its pathological significance in temperate forests: a literature review. *Forestry*, 74(4):319–336. doi: 10.1093/forestry/74.4.319.

Vospernik, S., 2006. Probability of bark stripping damage by red deer (*Cervus elaphus*) in Austria. *Silva Fennica*, 40(4): 589–601. doi: 10.14214/sf.316.

Wam, H. K. and Hofstad, O., 2007. Taking timber browsing damage into account: A density dependant matrix model for the optimal harvest of moose in Scandinavia. *Ecol. Econ.*, 62(1):45–55. doi: 10.1016/j.ecolecon.2007.01.001.

Ward, A. I., White, P. C. L., Smith, A., and Critchley, C. H., 2004. Modelling the cost of roe deer browsing damage to forestry. *For. Ecol. Manage.*, 191(1):301–310. doi: 10.1016/j.foreco.2003.12.018.

Weisberg, P. J., Hadorn, C., and Bugmann, H., 2003. Predicting understorey vegetation cover from overstorey attributes in two temperate mountain forests. *Forstwissenschaftliches Centralblatt*, 122(5):273–286. doi: 10.1007/s10342-003-0004-4.

Widén, A., Jarnemo, A., Månsson, J., Lilja, J., Morel, J., and Felton, A. M., 2022. Nutrient balancing or spring flush – What determines spruce bark stripping level by red deer? *For. Ecol. Manage.*, 520. doi: 10.1016/j.foreco.2022.120414.

Zimová, S., Dobor, L., Hlásny, T., Rammer, W., and Seidl, R., 2020. Reducing rotation age to address increasing disturbances in Central Europe: potential and limitations. *For. Ecol. Manage.*, 475:1–14. doi: 10.1016/j.foreco.2020.118408.